TMR-Sensor-Array-Based Misalignment-Tolerant Wireless Charging Technique for Roadway Electric Vehicles

Xuyang Liu[1], Chunhua Liu[2], and Philip W. T. Pong[1]

[1]Department of Electrical and Electronic Engineering, The University of Hong Kong, Hong Kong
[2]School of Energy and Environment, City University of Hong Kong, Hong Kong

The wirelessly transferred power as well as charging efficiency will significantly drop due to the large misalignment between the transmitting coil and receiving coil for roadway electric vehicles (EVs). A low-cost and reliable misalignment-tolerant wireless charging technique is indispensable for the rapid commercialization of wireless EV charging. This paper presents a technique to achieve the misalignment-tolerant wireless charging for the dynamic wireless charging (DWC) system by means of a tunneling magnetoresistive (TMR) sensor array as well as the easy-to-fabricate receiving coils. The TMR sensor array provides the coil-misalignment position by measuring the magnetic field component generated from the transmitting coil. The corresponding receiving coils are selected to be in resonance according to the measured coil-misalignment positions. In this paper, a sensor array composed of 29 uniaxial TMR sensors was utilized to measure the magnetic field component. This effectiveness of the proposed technique has been validated by both the finite-element method (FEM) simulations and laboratory experiments. The experimental results demonstrated that the proposed misalignment-tolerant wireless charging system can operate in a relatively wide misalignment range of ±120 mm with charging efficiency higher than 76.2%.

***Index Terms*— Coil-misalignment tolerant, dynamic wireless charging (DWC), magnetic field measurement, tunneling magnetoresistive (TMR) sensor array.**

I. Introduction

THE inductive power transfer (IPT) technology using magnetic resonance for wireless electric vehicle (EV) charging has attracted considerable attention since it enables the dynamic wireless charging (DWC) of a roadway EV [1]–[3]. However, the misalignment tolerance between the vehicle-mounted receiving coil and ground-embedded transmitting coil is still a challenging problem for the commercialization of wireless EV charging [4]. The charging power and efficiency will drop due to the lateral coil misalignment which easily occurs in the practical driving situations.

Previous researches on the misalignment-tolerant wireless power transfer (WPT) technique can be summarized into the following. Specially made coils with structures of Double and Quad D Quadrature [5]–[7] were proposed to maximum the misalignment-tolerance, whereas this method highly relies on the complex procedure of coil manufacture and requires specially built power electronic circuits. The autonomous coil alignment system (ACAS) achieves the misalignment adjustment by detecting the misalignment and then adjusting the coil positions [8]–[11]; however, it suffers from high cost and complicated operation of coil adjustment system for EVs such as by means of servo motors.

To overcome the constraints of the above-mentioned technique, a tunneling magnetoresistive (TMR) sensor-array-based misalignment-tolerant wireless charging system for roadway EVs is proposed in this paper, which makes use of the easy-to-fabricate coil design and low-cost TMR sensor array. TMR sensors have been widely used in magnetic field measurement applications such as in EVs due to their advantages such as low cost, compact size, high sensitivity, wide operating bandwidth, and low power consumption [12]–[14]. The TMR sensor array is placed on the same plane of receiving coils to detect the magnetic field generated from the transmitting coil, which has been validated to detect the coil misalignment accurately [15]. Different from the traditional receiving coil design, this paper uses three overlapping receiving coils of the same structure. The receiving coils are selected to be in resonance according to the measured misalignment. Therefore, the wireless charging system can provide relatively high transferred power with high charging efficiency in a wide misalignment range.

This paper is organized as follows. Section II presents the operating principle of coil-misalignment determination and the misalignment-tolerant wireless charging. The 3-D finite-element method (FEM) simulations were performed to verify the proposed technique in Section III. The experimental preparation including experimental prototype implementation and TMR sensor array pre-calibration is presented in Section IV. Section V demonstrates the experimental results. Section VI finally addresses the conclusion.

II. Operating Principles

The operation of the traditional IPT technology resembles a coupled transformer, represented as the equivalent circuit of Fig. 1(a) and structure of Fig. 1(b). The power is wirelessly transferred through the IPT mechanism when the transmitting coil and receiving coil are in resonance. However, the wireless transferred power will significantly drop when there exists a large misalignment as the mutual inductance (M_{tr}) as well as the coupling coefficient between the transmitting coil

Manuscript received November 5, 2018; accepted March 5, 2019. Corresponding authors: C. Liu and P. W. T. Pong (e-mail: chunliu@cityu.edu.hk; ppong@eee.hku.hk).

Color versions of one or more of the figures in this paper are available online at http://ieeexplore.ieee.org.

Digital Object Identifier 10.1109/TMAG.2019.2903895

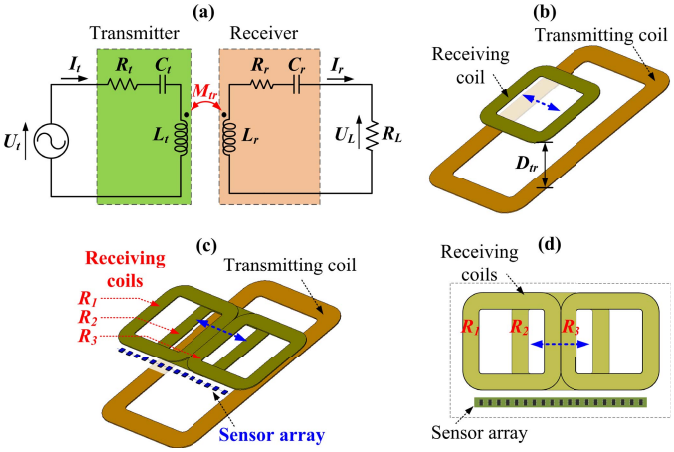

Fig. 1. (a) Schematic circuit of the traditional wireless charging system. (b) Structure of the traditional wireless charging system. (b) Structure of the proposed wireless charging system. (c) Top view of the receiver with sensor array.

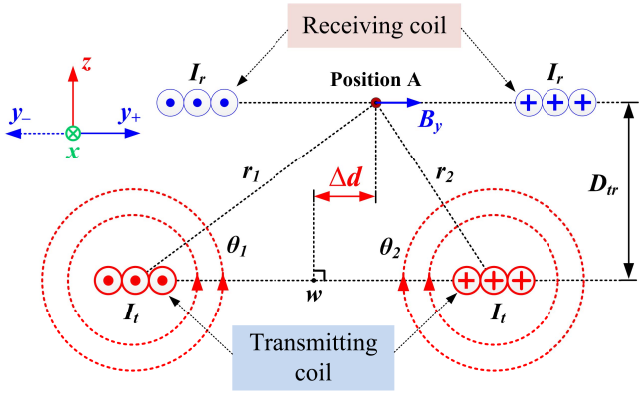

Fig. 2. Diagram of the magnetic field B_y distribution.

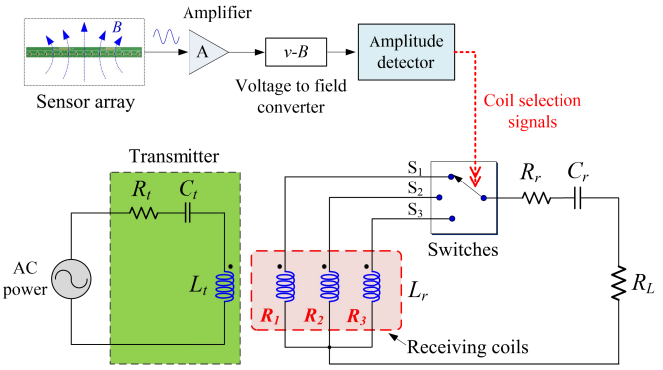

Fig. 3. Operating schematic of the misalignment-tolerant wireless charging system with the TMR sensor array.

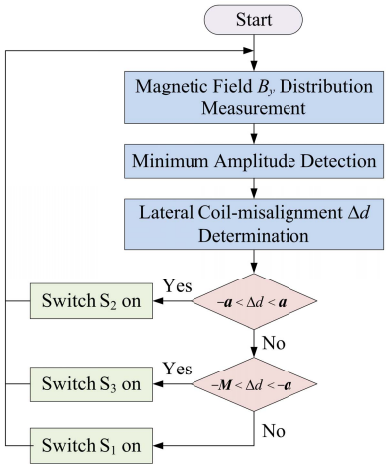

Fig. 4. Flowchart showing the operating principle.

and receiving coil decrease. To overcome such a constraint, a misalignment-tolerant wireless charging system is proposed in this paper, as depicted in Fig. 1(c) and (d). Different from the traditional receiver structure, the proposed receiver is composed of three overlapping receiving coils and a TMR sensor array at the same plane.

A. Coil-Misalignment Determination

The marker-free coil-misalignment determination is achieved using a TMR sensor array. The TMR sensor array is placed at the same plane of the receiving coils to detect the y-axis component of the magnetic field (B_y). As depicted in Fig. 2, B_y at the position A can be approximately calculated according to the Biot–Savart law [8], [15]

$$B_y = \frac{n\mu_0 I_t}{2\pi}\left(\frac{\sin\theta_1}{r_1} - \frac{\sin\theta_2}{r_2}\right) \quad (1)$$

where I_t is the current through the transmitting coil, μ_0 is the vacuum permeability, n is the turn number of the transmitting coil, r_1 and r_2 are the distances between the transmitting coil and position A, and θ_1 and θ_2 are the angles between the plane of the transmitting coil and the lines connecting position A to transmitting coil. From (1), there exists a sensing position where the magnitude of B_y is minimum at nearly 0. The lateral misalignment of the receiving coil will result in the lateral shift of B_y distribution. Therefore, lateral coil misalignment along the y-axis direction can be determined by detecting the sensing position, where B_y is minimum at nearly 0.

B. Misalignment-Tolerant Wireless Charging

As the wirelessly transferred power depends on the position of receiving coil of the traditional WPT technique, three overlapping receiving coils on the receiver side are employed to absorb the transferred power individually and then to eliminate the coil-misalignment effect. The receiving coils are selected to be in resonance with the transmitting coil according to the measured coil-misalignment position by the TMR sensor array, as presented in Fig. 3.

Fig. 4 shows the flowchart of the operating principle. Here, $\boldsymbol{M}$ denotes the maximum operating misalignment range. When the coil misalignment (Δd) is in the range of $\pm\boldsymbol{a}$, the receiving coil R_2 is connected to the compensation capacitor in order to absorb the maximum power; whereas when Δd is in the range between $-\boldsymbol{a}$ and $-\boldsymbol{M}$, the receiving coil R_3 is connected to the compensation capacitor. Similarly, the receiving coil R_1 is selected when Δd is in the range between $+\boldsymbol{a}$ and $+\boldsymbol{M}$. The value of $\boldsymbol{a}$ depends on the size of the receiving coil, which can be determined by the FEM simulation and experiments.

TABLE I
PARAMETERS OF IPT-BASED WPT SYSTEM IN FEM SIMULATIONS

Parameter	Symbol	Value
Transmitting coil inductance	L_t	247.28 μH
Transmitting coil internal resistance	R_t	0.346 Ω
Transmitting coil number of turns	N_1	20
Transmitting coil compensation capacitor	C_t	0.256 μF
Receiving coil R_1 inductance	L_{R1}	63.48 μH
Receiving coil R_2 inductance	L_{R2}	63.19 μH
Receiving coil R_3 inductance	L_{R3}	63.58 μH
Receiving coil R_1 internal resistance	R_{R1}	0.1382 Ω
Receiving coil R_2 internal resistance	R_{R2}	0.1375 Ω
Receiving coil R_3 internal resistance	R_{R3}	0.1374 Ω
Receiving coils number of turns	N_2	15
Receiving coil compensation capacitor	C_r	0.565 μF
Current through transmitting coil	I_t	8 A_{RMS}
Load resistance	R_L	5.26 Ω
Vertical distance between coils	D_{tr}	60 mm
Operating frequency	f_s	20 kHz

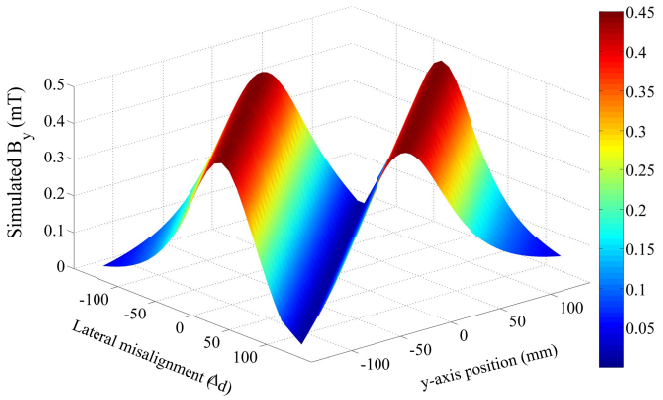

Fig. 5. Simulated y-axis components (B_y) versus Δd.

Therefore, it is feasible to provide higher transferred power using the proposed WPT technique by selecting the appropriate receiving coils to be in resonance.

III. FEM SIMULATIONS

To analytically verify the proposed misalignment-tolerant wireless charging system, 3-D FEM simulations were carried out using the commercial simulation software JMAG Designer 14. The main parameters of the WPT system are listed in Table I. The IPT-based WPT adopting series-series topology was used in the simulation, which operates in the resonance frequency of 20 kHz. It is worth noting that the proposed technique is applicable for the WPT with higher resonance frequency (e.g., more than 100 kHz) as TMR sensor can work in the wide bandwidth up to 1 MHz. In addition, the WPT in simulations operates in the constant-current mode with the current through the transmitting coil 8 A_{rms}.

The simulated y-axis component (B_y) of magnetic flux density under the misalignment (Δd) in the range of ± 120 mm is presented in Fig. 5. There exists the minimum flux density

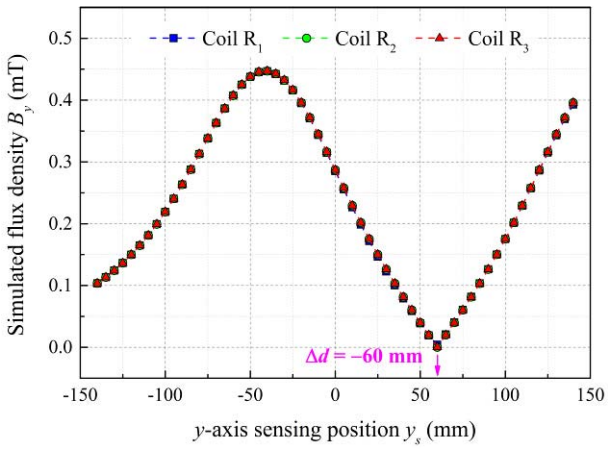

Fig. 6. Simulated y-axis components (B_y) with three receiving coils (i.e., R_1, R_2, and R_3) chosen in resonance individually when $\Delta d = -60$ mm.

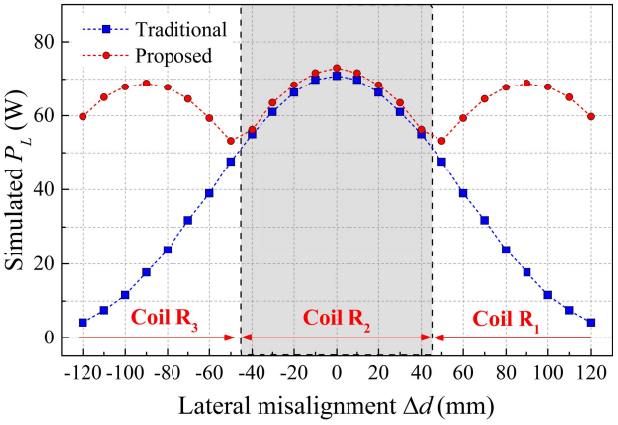

Fig. 7. Simulated transferred power (P_L).

at nearly 0 mT along the y-axis direction which agrees with (1). The position where the minimum amplitude exists will change corresponding to the lateral misalignment change. Thus, it is feasible to detect the minimum amplitude of the B_y distribution for determining Δd.

The simulation result shows that the B_y distribution is independent of the selection of receiving coils. Fig. 6 shows the simulated flux densities B_y with three receiving coils (i.e., R_1, R_2, and R_3) selected in resonance with the transmitting coil individually when the lateral coil misalignment Δd is -60 mm. The flux densities B_y in Fig. 6 have nearly the same distribution, and they experience the same pattern where the minimum magnitude exists in the sensing position of 60 mm. The B_y distribution only depends on the lateral misalignment (Δd). Thus, the B_y distribution is feasible to be used to determine the lateral misalignment under variable selections of receiving coil.

The comparison between the simulated transferred power (P_L) using the proposed WPT technique and the traditional one is presented in Fig. 7. By selecting the receiving coils in resonance with the transmitting coil according to the lateral misalignment (Δd), the transferred power can remain at a relatively high level. When Δd is

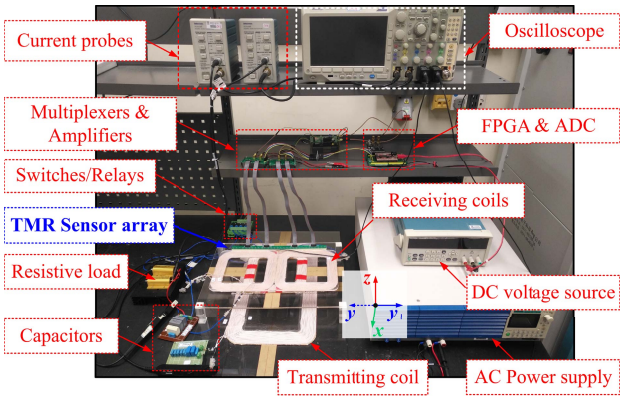

Fig. 8. Experimental prototype demonstrating the proposed WPT system.

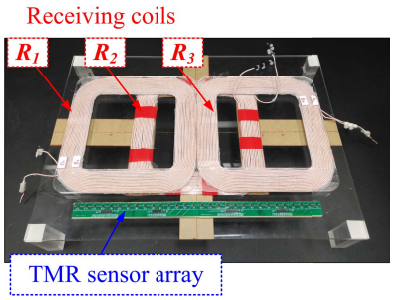

Fig. 9. Photograph of the proposed receiving coils with TMR sensor array.

in the range of ±40 mm, the receiving coil R_2 is selected in resonance, whereas when Δd is in the range between −40 and −120 mm, the receiving coil R_3 is selected accordingly. Similarly, when Δd is in the range between 40 and 120 mm, the receiving coil R_1 is selected. The proposed WPT technique can even provide the power of approximately 60 W when there exists a large misalignment of 120 mm, which accounts for 81.5% of the maximum power (i.e., when $\Delta d = 0$ mm). Therefore, the proposed technique can achieve misalignment-tolerant wireless charging.

IV. Experiments

A. Experimental Prototype

To experimentally validate the proposed WPT technique, a WPT prototype was built in the laboratory, as shown in Fig. 8. The transmitter and receiver in experiments were fabricated according to the simulation parameters as listed in Table I. The transmitter was powered by a constant current power source (PBZ40-10, Kikusui). The amplitude and frequency of current through the transmitting coil were kept constant at 8 A_{rms} and 20 kHz, respectively. The vertical distance between the transmitter and receiver was 60 mm. The currents through the transmitter and receiver in experiments were captured by two wideband current probes (TCPA300, Tektronix)

The receiver was composed of three overlapping receiving coils (i.e., R_1, R_2, and R_3) of the same structure, and a TMR sensor array was built in the laboratory, as shown in Fig. 9. The TMR sensor array consisting of 29 uniaxial TMR sensors uniformly distributed in an interval of 10 mm was placed on

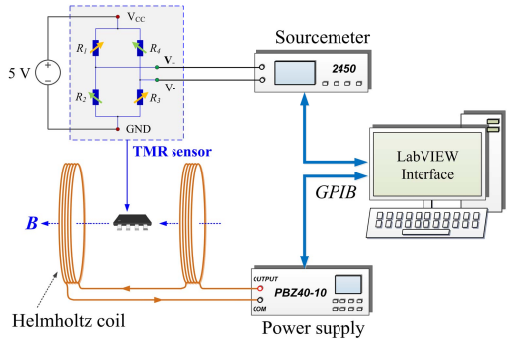

Fig. 10. Pre-calibration configuration for the uniaxial TMR sensor.

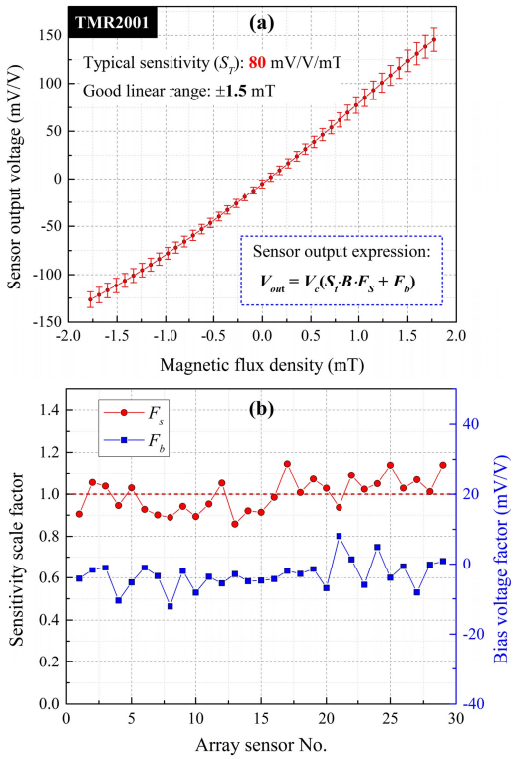

Fig. 11. (a) Pre-calibration results of the sensor array composed of 29 TMR sensors. (b) Sensitivity scale factors and bias voltage factors of TMR sensors.

the same place of the receiving coils. The height of the sensor array was kept the same as that of the receiving coils so that the sensor array only measured the y-axis component (B_y) of the magnetic field generated from the transmitting coil. The sensor array was powered by the constant voltage source (PWS2326, Tektronix). The outputs of the TMR sensor array were multiplexed by the differential multiplexers (ADG1606, Analog Devices) and then amplified by the instrument amplifier (AD620, Analog Devices). The amplified sensor output signals were then continuously sampled by the analog-to-digital converter (AD9226, Analog Devices) and a field-programmable gate array (FPGA) in a sampling rate of 5 MS/s. The minimum magnitude of sensor signals was analytically detected by the FPGA, and the lateral misalignment (Δd) was then determined. The coil selection signals were finally given by the FPGA according to the measured Δd.

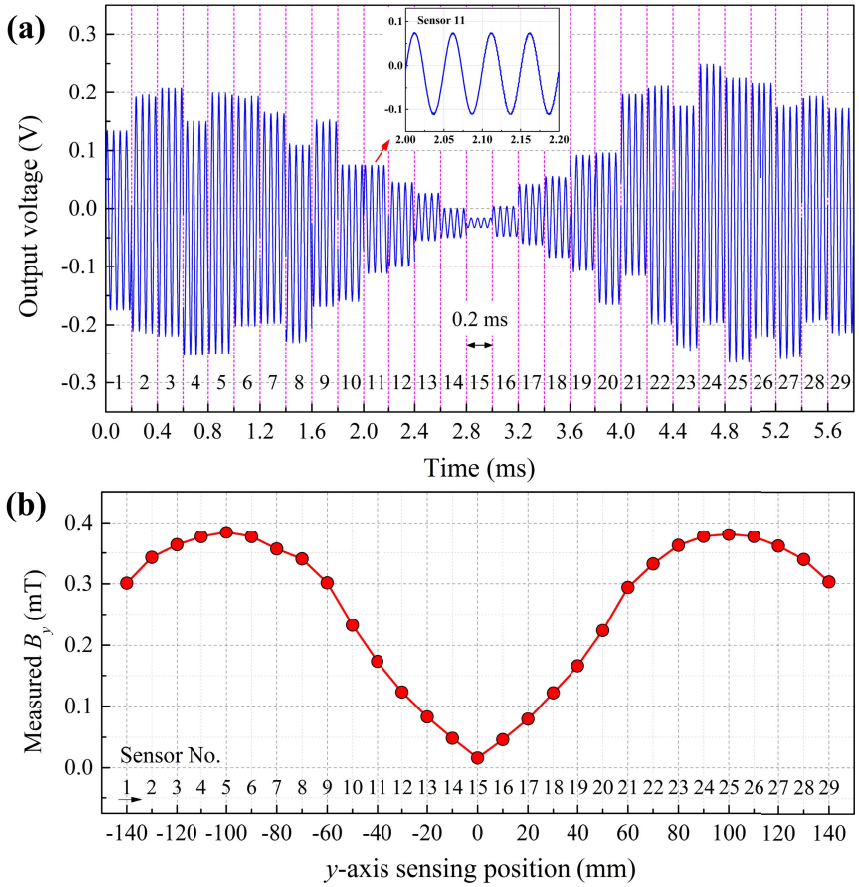

Fig. 12. (a) Measured sensor array output signals. (b) Measured y-axis component (B_y, rms value) of magnetic flux density.

B. Sensor Array Pre-Calibration

To precisely measure the y-axis component (B_y) of the magnetic field, each TMR sensor of the sensor array was pre-calibrated using a Helmholtz coil, as shown in Fig. 10. The pre-calibration process aimed to eliminate the slight field-to-voltage characteristic variation of the TMR sensors in experiments. The Helmholtz coil powered by a programmable current source provided the pre-determined vector magnetic field loop along the sensitive axis of the TMR sensor.

The TMR2001 sensor with unique Wheatstone bridge configuration was used in experiments, which generally work in a linear range of ±1.5 mT with typical sensitivity of 80 mV/V/mT [16]. The pre-calibration results of 29 TMR2001 sensors are summarized in Fig. 11. It is observed from Fig. 11(a) that the TMR sensors in sensor array suffered from the slightly different field-to-voltage characteristics even though they all experienced the good linearity. The sensor output of each TMR sensor can be expressed by a linear function as

$$V_{\text{out}} = V_c(S_t \cdot B \cdot F_s + F_b) \tag{2}$$

where V_c is the constant supply voltage, S_t is the sensor target sensitivity, B is the magnetic flux density to be measured, F_s is the sensitivity scale factor, and F_b is the bias voltage factor. All values of F_s and F_b shown in Fig. 11(b) were stored in a lookup table, which can be accessed by the FPGA to ensure the precise magnetic field measurement.

V. Experimental Results and Discussion

The experimental results are presented in this section to demonstrate the effectiveness of the proposed technique. The sensor array output signals as well as the y-axis component (B_y) of magnetic flux density were measured as presented in Fig. 12. It is observed from Fig. 12(a), sinusoidal voltage waveforms with a frequency of 20 kHz were generated by the TMR sensor array corresponding to the variable magnetic field. The sampling time for each sensor is 0.2 ms which equals four cycles of the variable magnetic field, as presented in the inset of Fig. 12(a). Even there exist different offsets among sensor outputs, by using the stored values of F_s and F_b, the rms value of B_y at the sensing positions in the range of ±140 mm can be precisely measured according to (2), as shown in Fig. 12(b).

By regulating the lateral coil-misalignment positions (Δd), the y-axis components (B_y) of magnetic flux density and current waveforms were measured under different misalignment conditions, as shown in Fig. 13. It is obverted from Fig. 13(a)–(e) that the B_y distribution varied corresponding to Δd. There exists a minimum amplitude at nearly 0 mT from the B_y distribution measured by the TMR sensor array. Thus, the value of Δd can be determined by detecting the minimum

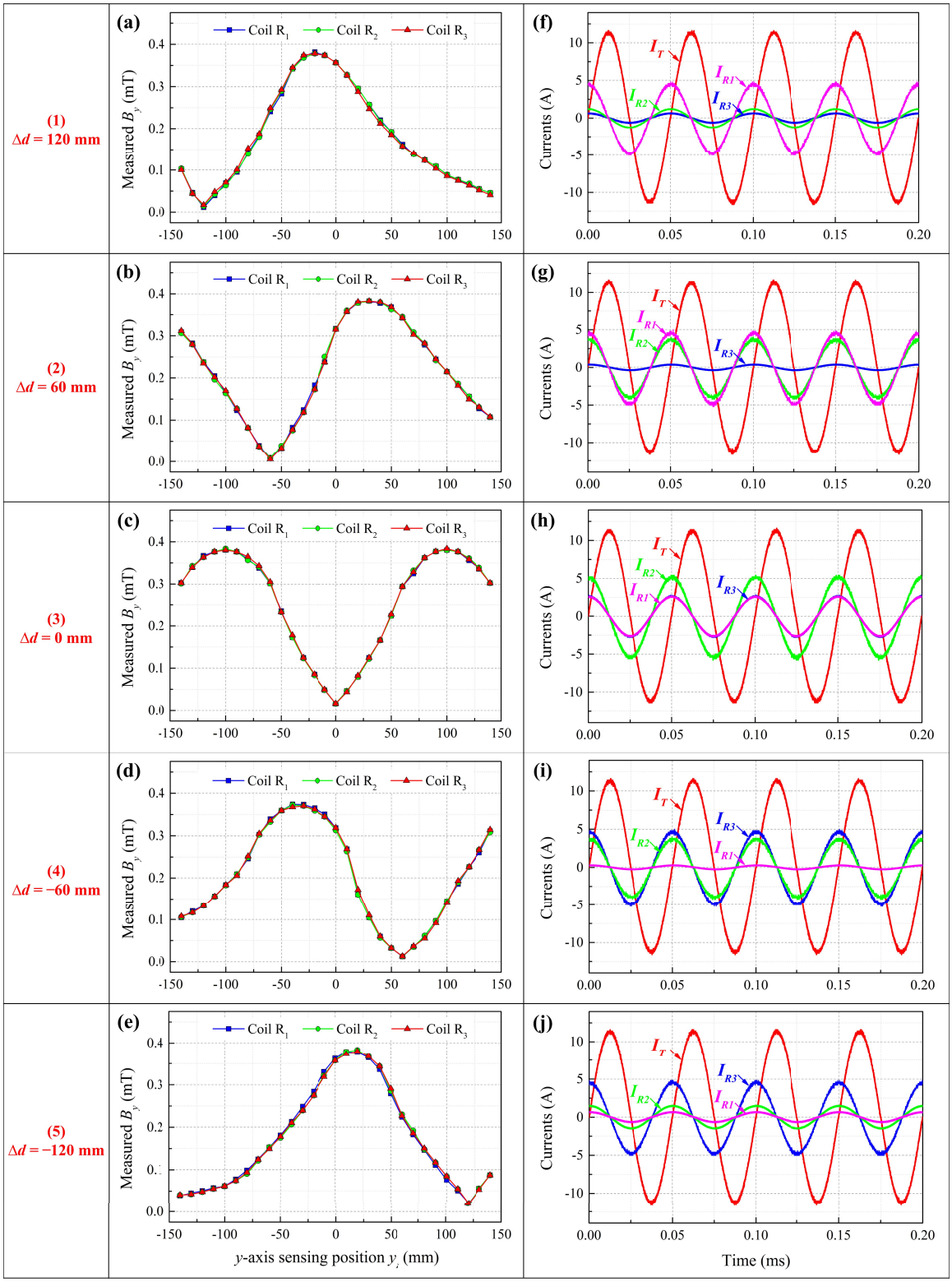

Fig. 13. Measured B_y in rms value and measured current waveforms under different misalignment conditions.

amplitude. It is also found that the measured B_y distribution is independent of the selection of the receiving coils in resonance with the transmitting coil. The B_y distribution only depends on the current through the transmitting coil (I_t) and Δd. As I_t is kept constant in experiments, therefore, the lateral misalignment can be accurately measured using the TMR sensor array. It is also worthwhile to state that more accurate misalignment determination can be obtained by using a sensor array with more sensors and the smaller interval between sensors.

It is found from Fig. 13(f)–(j) that the proposed WPT technique can ensure high transferred power by selecting the appropriate receiving coil to be in resonance. When Δd is

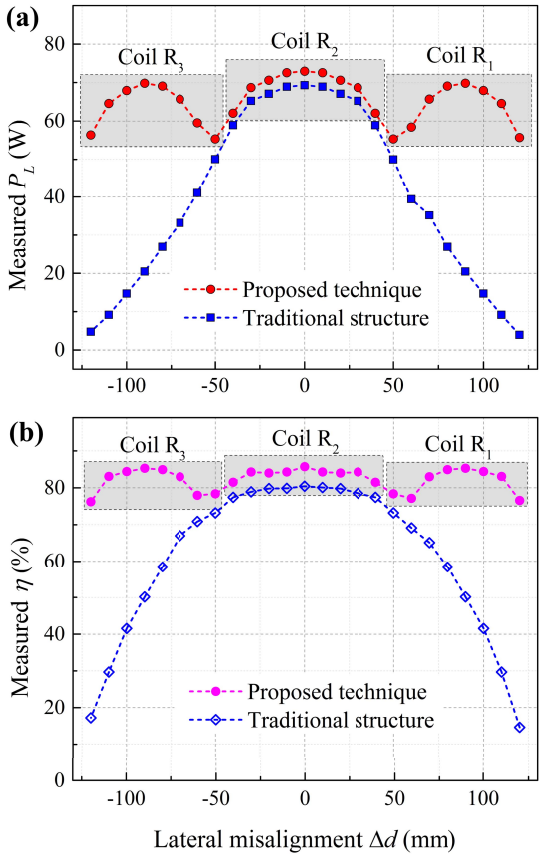

Fig. 14. (a) Measured transferred power (P_L) versus Δd. (b) Measured power transfer efficiency (η) versus Δd.

0 mm, the maximum current can be obtained by selecting receiving coil R_2, whereas the maximum current can be obtained by selecting coil R_1 when Δd becomes 60 and 120 mm. Similarly, the maximum current can be obtained by selecting coil R_3 when Δd changes into -60 and -120 mm. Thus, the higher transferred power can be ensured by selecting the appropriate receiving coil in resonance according to the measured Δd.

The WPT performances of the proposed technique and the traditional were also compared in experiments. The experimental results show that by selecting the appropriate receiving coil to be in resonance, higher transferred power (P_L) and higher power transfer efficiency (η) can be obtained in the misalignment range of ± 120 mm, as shown in Fig. 14. The proposed WPT technique can provide the transferred power of 55.6 W and power transfer efficiency of 76.2% even there exists a large misalignment of 120 mm, whereas the traditional one only provided the transferred power of 3.94 W and power transfer efficiency of 14.6%. Therefore, the proposed TMR-sensor-array-based WPT technique can achieve the misalignment-tolerant wireless charging in a relative wide misalignment range.

VI. Conclusion

This paper proposed a new TMR-sensor-array-based WPT technique to achieve the misalignment-tolerant wireless charging. Higher transferred power as well as wireless charging efficiency can be obtained using the cost-effective TMR-sensor-array and easy-to-fabricate receiving coils. This technique can provide sights to more flexible and easy-to-operate misalignment-tolerant wireless charging solution for the roadway EVs.

Acknowledgment

This work was supported in part by The University of Hong Kong through the Seed Funding Program for Basic Research, Seed Funding Program for Applied Research, and Small Project Funding Program, in part by the ITF Tier 3 Funding under Grant ITS/203/14, Grant ITS/104/13, and Grant ITS/214/14, in part by the RGC-GRF under Grant HKU 17210014 and Grant HKU 17204617, and in part by the University Grants Committee of Hong Kong under Contact AoE/P-04/08.

References

[1] G. A. Covic and J. T. Boys, "Inductive power transfer," *Proc. IEEE*, vol. 101, no. 6, pp. 1276–1289, Jun. 2013.
[2] S. Li and C. C. Mi, "Wireless power transfer for electric vehicle applications," *IEEE J. Emerg. Sel. Topics Power Electron.*, vol. 3, no. 1, pp. 4–17, Mar. 2015.
[3] S. Y. Choi, B. W. Gu, S. Y. Jeong, and C. T. Rim, "Advances in wireless power transfer systems for roadway-powered electric vehicles," *IEEE J. Emerg. Sel. Topics Power Electron.*, vol. 3, no. 1, pp. 18–36, Mar. 2015.
[4] Z. Bi *et al.*, "A review of wireless power transfer for electric vehicles: Prospects to enhance sustainable mobility," *Appl. Energy*, vol. 179, pp. 413–425, Oct. 2016.
[5] K. A. Kalwar, S. Mekhilef, M. Seyedmahmoudian, and B. Horan, "Coil design for high misalignment tolerant inductive power transfer system for EV charging," *Energies*, vol. 9, no. 11, p. 937, Nov. 2016.
[6] M. Budhia, J. T. Boys, G. A. Covic, and C.-Y. Huang, "Development of a single-sided flux magnetic coupler for electric vehicle IPT charging systems," *IEEE Trans. Ind. Electron.*, vol. 60, no. 1, pp. 318–328, Jan. 2013.
[7] M. M. Alam, S. Mekhilef, M. Seyedmahmoudian, and B. Horan, "Dynamic charging of electric vehicle with negligible power transfer fluctuation," *Energies*, vol. 10, no. 5, p. 701, May 2017.
[8] K. Hwang *et al.*, "Autonomous coil alignment system using fuzzy steering control for electric vehicles with dynamic wireless charging," *Math. Problems Eng.*, vol. 2015, Nov. 2015, Art. no. 205285.
[9] I. Cortes and W.-J. Kim, "Lateral position error reduction using misalignment-sensing coils in inductive power transfer systems," *IEEE/ASME Trans. Mechatronics*, vol. 23, no. 2, pp. 875–882, Apr. 2018.
[10] K. Hwang *et al.*, "An autonomous coil alignment system for the dynamic wireless charging of electric vehicles to minimize lateral misalignment," *Energies*, vol. 10, no. 3, p. 315, Mar. 2017.
[11] M. R. Barzegaran, H. Zargarzadeh, and O. A. Mohammed, "Wireless power transfer for electric vehicle using an adaptive robot," *IEEE Trans. Magn.*, vol. 53, no. 6, Jun. 2017, Art. no. 7205404.
[12] X. Liu, C. Liu, and P. W. T. Pong, "Velocity measurement technique for permanent magnet synchronous motors through external stray magnetic field sensing," *IEEE Sensors J.*, vol. 18, no. 10, pp. 4013–4021, May 2018.
[13] L. Jogschies *et al.*, "Recent developments of magnetoresistive sensors for industrial applications," *Sensors*, vol. 15, no. 11, pp. 28665–28689, Nov. 2015.
[14] P. Freitas *et al.*, "Magnetoresistive sensors," *J. Phy., Condens. Matter*, vol. 19, no. 16, 2007, Art. no. 165221.
[15] X. Liu, W. Han, C. Liu, and P. W. T. Pong, "Marker-free coil-misalignment detection approach using TMR sensor array for dynamic wireless charging of electric vehicles," *IEEE Trans. Magn.*, vol. 54, no. 11, Nov. 2018, Art. no. 4002305.
[16] *TMR2001 TMR Linear Sensor Datasheet*. Accessed: Nov. 2018. Tech. Rep. TMR2001. [Online]. Available: http://www.dowaytech.com/en/1944.html